# Crystallization behavior and mechanical properties of nano-CaCO3/beta-nucleated ethylene-propylene random copolymer composites

Mai J. H., Zhang M. Q., Rong M. Z., Bárány T., Ruan W. H.

Accepted for publication in Express Polymer Letters
Published in 2012
DOI: 10.3144/expresspolymlett.2012.79

eXPRESS Polymer Letters Vol.6, No.9 (2012) 739–749
Available online at www.expresspolymlett.com
DOI: 10.3144/expresspolymlett.2012.79

# Crystallization behavior and mechanical properties of nano-$CaCO_3$/β-nucleated ethylene-propylene random copolymer composites

*J. H. Mai*[1,2], *M. Q. Zhang*[1], *M. Z. Rong*[1], *T. Bárány*[3], *W. H. Ruan*[1,2*]

[1]Materials Science Institute, Sun Yat-sen (Zhongshan) University, 510275 Guangzhou, China
[2]Key Laboratory for Polymeric Composite and Functional Materials of Ministry of Education, DSAPM Lab, School of Chemistry and Chemical Engineering, Sun Yat-sen (Zhongshan) University, 510275 Guangzhou, China
[3]Department of Polymer Engineering, Faculty of Mechanical Engineering, Budapest University of Technology and Economics, Műegyetem rkp. 3., H-1111 Budapest, Hungary

*Received 11 December 2011; accepted in revised form 8 April 2012*

**Abstract.** To provide ethylene-propylene random copolymer (PPR) with balanced mechanical properties, β-nucleating agent and $CaCO_3$ nanoparticles are incorporated into PPR matrix by melt blending. It is found that crystallization rate and relative content of β-crystal increase with the addition of β-nucleating agent together with nanoparticles. Size of PPR spherulite is greatly reduced, and a specific morphology appears, in which α-crystal lamella is grown upon the β-nucleus. The results suggest that both β-nucleating agent and nano-$CaCO_3$ have heterogeneous nucleation and synergistic effects on β-nucleation of PPR. Mechanical characterization shows that mechanical properties of PPR can be tuned by incorporation of β-nucleating agent and nano-$CaCO_3$ particles. Under suitable compositions, low temperature impact strength and high temperature creep resistance of PPR, the bottlenecks of application of such material, can be simultaneously improved without sacrificing the Youngs'modulus and tensile strength.

***Keywords:*** *mechanical properties, ethylene-propylene random copolymer, β-nucleating agent, nano-$CaCO_3$, crystallization*

## 1. Introduction

As one of the most popular commodity plastics, polypropylene (PP) is facing the challenge of improving its mechanical properties to meet versatile application requirements. Accordingly, random copolymers of propylene with a low amount of 1-olefins such as ethylene, 1-butene, 1-hexene and 1-octane are synthesized. Among these copolymers, ethylene-propylene random copolymer (PPR) has received a great deal of attentions owing to its higher impact strength than isotactic PP [1]. It has been used for making pipes, plates, domestic appliances and automobiles. However, the introduction of ethylene units leads to lower crystallization temperature and degree of crystallinity of the polymer. Meanwhile, stiffness, strength, creep properties and thermal deformation temperature of PPR also decrease. Low temperature impact strength of such materials is still poor, causing problems for parts assembling and potential safety hazards. In this context, modification of PPR is necessary for acquiring balanced mechanical properties. Considering that crystalline morphology and degree of crystallinity determine structure and properties of semi-crystalline polymers [2], improving of overall performance of PPR had better to start with crystallization aspects.

So far as we know, toughness and thermal deformation temperature of β-form isotactic polypropylene

---

[*]Corresponding author, e-mail: cesrwh@mail.sysu.edu.cn

(iPP) are much higher than that of α-form iPP [3–10]. However, β-modification contingently occurs in commercial PP and can only be formed under critical conditions like large temperature gradient [11, 12], shearing the melt [13, 14] or adding selective β-nucleating agent (β-NA) [15]. Comparatively, the addition of specific nucleating agents is the most reliable method for the preparation of the beta-form PP [15]. It would increase crystallization temperature and degree of crystallinity of iPP, and accelerates the crystallization rate.

Additionally, incorporation of nanometer-scale inorganic particles is a promising approach to improve both mechanical and thermal properties of polymeric materials. It was reported that when nano-$CaCO_3$ particles were added to iPP, not only modulus and toughness of the matrix were significantly improved [16], but also β-crystals were formed [17].

Although most available documents deal with β-nucleatd i-PP modification, and few have paid attention to random polypropylene copolymer [18–25], the results are meaningful. Considering that nano-$CaCO_3$ have applications in PPR products, and gaining enlightenment from the studies on filled β-nucleated iPP [26–30], we plan to add β-nucleating agent and $CaCO_3$ nanoparticles into PPR together. Crystalline characteristics, structure and mechanical properties of PPR composites prepared under processing conditions will be studied. It is hoped that synergistic effect would appear, overcoming the above-mentioned shortcomings of PPR. Furthermore, knowledge of structure and properties adjustment of PPR can be acquired. These are the objectives of the present work.

## 2. Experimental

### 2.1. Materials

Ethylene-propylene random copolymer (trade name: PPR4220; MFI = 0.25 g/10 min at 230°C and 2.16 kg, content of ethylene is approximately 5.0 mol% and the molecular weight distribution is approximately 4.0) was supplied by Yanshan Petrochemical Co., Beijing, China. The rare-earth β-nucleating agent (trade name WBG-II, which is a heteronuclear dimetal complex of lanthanum and calcium with some specific ligands) was obtained from Guangdong Winner Functional Materials Co., Ltd. Foshan, China. A commercial grade of active calcium carbonate nanoparticles surface pre-treated by stearic acid (with average size of 30 nm, content of $CaCO_3 \geq 95\%$ and pH = 8.5~10.5) were obtained from Henan Keli New Material Co., Ltd. Xuchang, China.

### 2.2. Sample preparation

Before melt mixing, PPR and nano-$CaCO_3$ particles were dried at 60°C for 12 h. The β-nucleating agent and nanofillers were blended with PPR under certain proportions in a Haake mixer (Rheocord 300p, Haake, Germany) at 180°C and 60 rpm for 10 min. For comparsion, β-nucleating agent/PPR and nano-$CaCO_3$/PPR composites were prepared under same ways. Then, the compounds were broken and injection molded into standard bars for mechanical tests by a vertical injection molding machine (Y-350, Yida Co., Ltd, China) at barrel temperature of 210°C. Prior to the tests, samples were conditioned at room temperature (23±2°C) and relative humidity of 50±5% for 48 h.

### 2.3. Characterization

Non-isothermal melting and crystallization behaviors of PPR and its composites were tested by differential scanning calorimeter (DSC) (MDSC2910, TA, USA) with nitrogen as purge gas. Pure indium and zinc were used as standard materials to calibrate both the temperature scale and melting enthalpy. All the samples for DSC measurements were cut from injection molded bars. For each measurement, sample was heated up to 200°C and maintained at this temperature for 5 min to eliminate thermal history. Afterwards, the sample was cooled down to 50°C and reheated to 200°C again. Both heating and cooling rates were 10°C/min.

Wide angle X-ray diffraction (WAXD,) pattern of the materials was collected at room temperature by a diffractometer (D-max 2200 VPC, Rigaku, Japan) with Cu $K_\alpha$ radiation. The X-ray source was set at voltage of 40 kV and current of 30 mA in a range of $2\theta$ = 5–35°, with a scanning rate of 5°/min. All the samples for WAXD measurements were cut from injection molded bars. The dimension of samples is $10\times10\times2$ mm.

A Leitz polarized light microscopy (PLM) (Orthoplan Pol, Leitz, German) with heating stage (THMS600, Linkam, England) was used for morphology observation. The sample sliced to thickness of 10–20 μm was firstly heated to 230°C, kept for 5 min to eliminate thermal history, and slided into a chamber set at the predetermined crystallization temperature of 130°C until completion of crystallization. In addition, morphological change during heating (heating rate = 0.1°C/min) was observed. The images presented in this paper were taken under orthogonally polarized condition.

Tensile test was conducted on ASTM D638-98 Type V specimens using a universal testing machine (H10K-S, Hounsfield, England) at a crosshead speed of 2 mm/min for Young's modulus and 50 mm/min for tensile strength under room temperature. Notched Charpy impact strengths of the specimens were measured at room temperature and –10°C according to ISO 179-2 by an advanced pendulum impact device (ATLAS, America) at a rate of 3.8 m/s. The specimens (size: $80\times10\times4$ mm$^3$) were notched with an automatic sample notcher (ASN, Dynisco instrumants, USA). An initial crack length of 2 mm and a span of 40 mm were selected. Five specimens were tested for each group of specimens.

Creep resistance of PPR and its composites was determined at 70°C under constant stress of 1 MPa and static force of 0.1 N with a dynamic mechanical analysis instrument (DMA2980, TA, USA), using three-point bending mode. The specimen size was $55\times10\times3$ mm$^3$.

## 3. Results and discussion

### 3.1. Non-isothermal crystallization and melting behaviors

Since PPR is mostly processed under non-isothermal conditions, study of its non-isothermal crystallization and melting behaviors is of great technological significance. Figures 1 shows the cooling and heating traces of PPR and its composites measured by DSC. The corresponding characteristic parameters are summarized in Table 1.

For pristine PPR, the temperature at which the crystallization curve starts to deviate from the baseline, $T_c^i$, peak temperature of crystallization, $T_c^p$, and onset temperature of crystallization, $T_c^{on}$, are 111.1, 103.0 and 106.3°C, respectively (Figure 1a). When a small amount of β-nucleating agent, nano-$CaCO_3$ or nano-$CaCO_3$/β-nucleating agent is added, the values of $T_c^i$, $T_c^p$ and $T_c^{on}$ of the composites become higher than those of PPR, and the increment amplitudes are about 10°C for β-nucleating agent or nano-$CaCO_3$/β-nucleating agent added systems. It means that β-nucleating agent and $CaCO_3$ nanoparticles have heterogeneous nucleation effects on PPR, and nucleation of β-nucleating agent is more effective than that of nano-$CaCO_3$.

Careful analysis of the data in Table 1 reveals that the addition of β-nucleating agent increases the half width of the crystallization peak in the high temperature region, $\Delta T_1$, and reduces the slope of the high-temperature side of exotherm, $S_i$, of PPR. On the contrary, $\Delta T_1$ of composites decreases, and $S_i$ increases when the nano-$CaCO_3$ added alone. In fact, the two parameters of $\Delta T_1$ and $S_i$ are closely related to crystal growth rate [31]. The higher $\Delta T_1$ and smaller $S_i$, the lower crystal growth rate is. From Table 1 it is also noted that when nano-$CaCO_3$/β-nucleating agent are incorporated to PPR, $S_i$ values of the composites are smaller, and $\Delta T_1$ values are also higher than those of β-nucleated PPR. Evidently, the rate of crystal growth of PPR increases with the addition of nano-$CaCO_3$, but decreases with the addition of β-nucleating agent or β-nucleating agent/nano-$CaCO_3$. So far as we know, for the given random

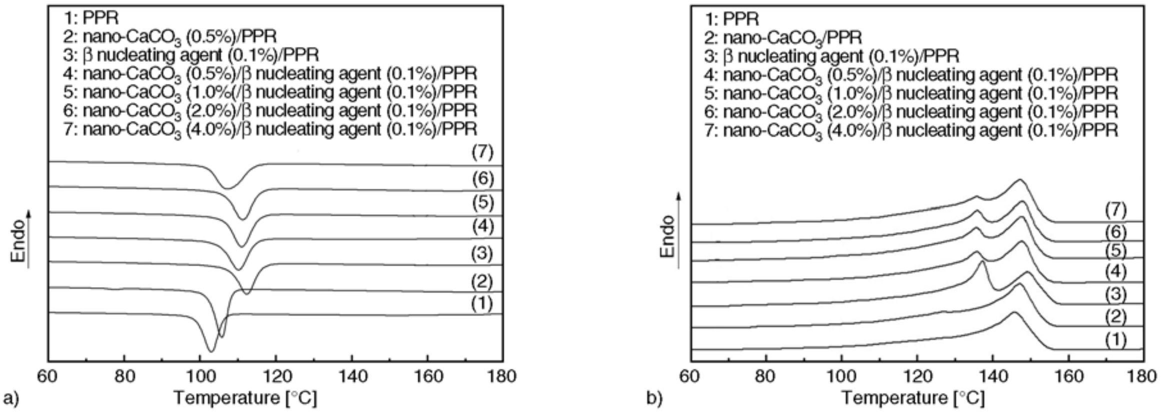

**Figure 1.** (a) DSC cooling and (b) heating curves of PPR and its composites

**Table 1.** Non-isothermal crystallization and melting data of PPR and its composites obtained from DSC

| Samples | $^aT_c^i$ [°C] | $^bT_c^p$ [°C] | $^cT_c^{on}$ [°C] | $^d\Delta T_1$ [°C] | $^e\Delta T_2$ [°C] | $^fS_i$ | $^gT_m^\alpha$ [°C] | $^hT_m^\beta$ [°C] | $^iT_m^i$ [°C] |
|---|---|---|---|---|---|---|---|---|---|
| PPR | 111.1 | 103.0 | 106.3 | 3.3 | 42.5 | 0.51 | 145.6 | – | 142.7 |
| β-NA (0.1 wt%)/PPR | 123.8 | 112.4 | 116.4 | 4.0 | 24.9 | 0.34 | 149.1 | 137.3 | 132.3 |
| β-NA (0.2 wt%)/PPR | 124.7 | 112.5 | 116.7 | 4.2 | 24.7 | 0.32 | 149.0 | 137.2 | 133.0 |
| β-NA (0.3 wt%)/PPR | 124.7 | 111.7 | 116.1 | 4.4 | 25.3 | 0.30 | 149.0 | 137.1 | 133.1 |
| β-NA (0.5 wt%)/PPR | 125.2 | 112.9 | 117.7 | 4.8 | 24.2 | 0.27 | 148.8 | 137.1 | 133.1 |
| 0.5 wt% $CaCO_3$/PPR | 113.9 | 105.8 | 108.3 | 2.5 | 41.2 | 0.87 | 147.0 | – | 142.3 |
| 1.0 wt% $CaCO_3$/PPR | 114.1 | 105.9 | 108.2 | 2.3 | 40.7 | 0.94 | 146.6 | – | 143.1 |
| 2.0 wt% $CaCO_3$/PPR | 114.0 | 105.6 | 108.2 | 2.6 | 41.4 | 0.86 | 147.0 | – | 141.9 |
| 4.0 wt% $CaCO_3$/PPR | 113.9 | 105.9 | 108.3 | 2.4 | 40.9 | 0.81 | 146.8 | – | 142.1 |
| Nano-$CaCO_3$ (0.5 wt%)/β-NA (0.1 wt%)/PPR | 120.8 | 110.2 | 114.7 | 4.5 | 25.7 | 0.29 | 147.6 | 135.9 | 132.5 |
| Nano-$CaCO_3$ (1.0 wt%)/β-NA (0.1 wt%)/PPR | 124.7 | 111.0 | 115.5 | 4.5 | 24.5 | 0.30 | 147.5 | 135.6 | 132.6 |
| Nano-$CaCO_3$ (2.0 wt%)/β-NA (0.1 wt%)/PPR | 126.2 | 111.3 | 115.8 | 4.5 | 24.7 | 0.30 | 147.7 | 135.9 | 133.0 |
| Nano-$CaCO_3$ (4.0 wt%)/β-NA (0.1 wt%)/PPR | 125.3 | 107.3 | 114.3 | 7.0 | 28.3 | 0.17 | 147.2 | 135.6 | 133.0 |

$^aT_c^i$: the temperature at which exothermic curve starts to deviate from the baseline
$^bT_c^p$: peak temperature of crystallization
$^cT_c^{on}$: onset temperature of crystallization
$^d\Delta T_1 = T_c^{on} - T_c^p$: half width of crystallization peak in the high temperature region
$^e\Delta T_2 = T_m^p - T_c^p$: degree of supercooling
$^fS^i$: slope of high-temperature side of exotherm
$^gT_m^\alpha$: peak temperature of melting of α crystal
$^hT_m^\beta$: peak temperature of melting of β crystal
$^iT_m^i$: initial melting temperature

copolymer in a wide temperature range, growth rate of β-phase crystal is lower than that of α-phase [15, 21, 23]. Therefore, the decrease of crystal growth rate of β-nucleating agent/PPR might be caused by generation of β-phase crystal. The obviously lower $S_i$ values of the composites containing both β-nucleating agent and nano-$CaCO_3$ indicate that the two components exert synergistic effect on inducing the formation of β-crystal of PPR.

On the other hand, the degree of supercooling, $\Delta T_2$, which characterizes the overall rate of crystallization, decreases with the addition of β-nucleating agent or nano-$CaCO_3$/β-nucleating agent, demonstrating that the rates of crystallization of the composites are still higher than that of PPR. It is known that crystallization includes nucleation and crystal growth. In the above discussion, it was found that crystal growth rates of β-nucleated PPR and nano-$CaCO_3$/β-nucleated PPR are lower than that of PPR, while the higher rate of crystallization hints effective heterogeneous nucleation effects of β-nucleating agent and nano-$CaCO_3$/β-nucleating agent on PPR.

Similarly, melting behavior of PPR is largely affected by the incorporation of β-nucleating agent and nano-$CaCO_3$/β-nucleating agent (Figure 1b). In the case of pristine PPR, there is only a single melting peak on the heating curve with peak temperature of 145.6°C, which is much lower than that of isotatic PP due to the random embedment of ethylene units. For nano-$CaCO_3$/PPR, a single melting peak on the heating curve with peak temperature around 147°C appears. When β-nucleating agent or nano-$CaCO_3$/β-nucleating agent is added into PPR, two endothermic peaks appear: one around 148°C and another around 136°C. Considering the lower melting temperature of β-crystal than that of α-crystal [15], the melting peak in the higher temperature regime should represent melting of α-crystal, and the one in the lower temperature regime should result from melting of β-crystal. The increase of $T_m^\alpha$ and appearance of $T_m^\beta$ with the addition of β-nucleating agent and nano-$CaCO_3$/β-nucleating agent prove heterogeneous nucleation and β-crystal formation.

## 3.2. Crystalline characteristics

Figure 2 shows WAXD spectra of PPR and its composites. For the spectrum of PPR, the most intense reflections are present at $2\theta$ of 14.0, 16.8, 18.6, 21.2 and 21.9°, corresponding to (110), (040), (130), (111) and (131) lattice planes of the most common α-monoclinic crystal. There is no new peak appearing in the spectra of nano-$CaCO_3$/PPR, meaning that $CaCO_3$ nanoparticles used actually have no β-nucle-

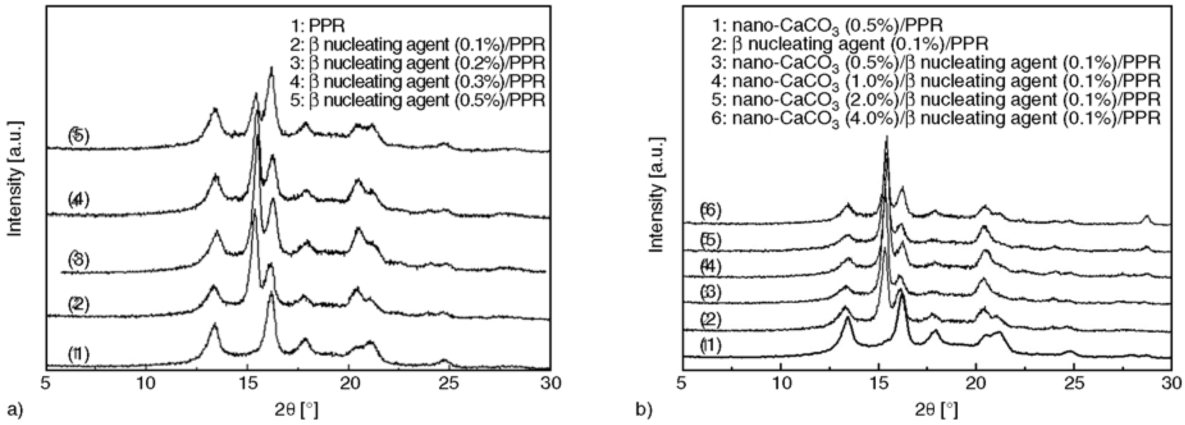

**Figure 2.** WAXD spectra of PPR and its composites a) β-nucleating/PPR systems, b) nano/$CaCO_3$/β-nucleating/PPR systems

ating effect on PPR. For the spectra of β-nucleated PPR and nano-$CaCO_3$/β-nucleated PPR, a new peak at $2\theta$ of around 16.0° is observed. It is assigned to (300) lattice plane of β-crystal, indicating the existence of β-crystal in PPR composites. There may also be (301) reflection of β-crystal at 21.2°, which overlaps (111) reflection of α-crystal.

By using peak intensity of (300) reflection, the relative proportion of the β-crystal, $K_\beta$, can be calculated according to the empirical Equation (1) of Turner-Jones *et al.* [32]:

$$K_\beta = \frac{I_{(300)}}{I_{(110)} + I_{(040)} + I_{(130)} + I_{(300)}} \quad (1)$$

where $I_{(300)}$ is the intensity of the (300) diffraction peaks of the WAXD patterns and $I_{(110)}$, $I_{(040)}$, $I_{(130)}$ are the intensities of the (110), (040), and (130) diffraction peaks, respectively. The calculated values of $K_\beta$ were plotted as a function of contents of β-nucleating agent and nano-$CaCO_3$ (Figure 3).

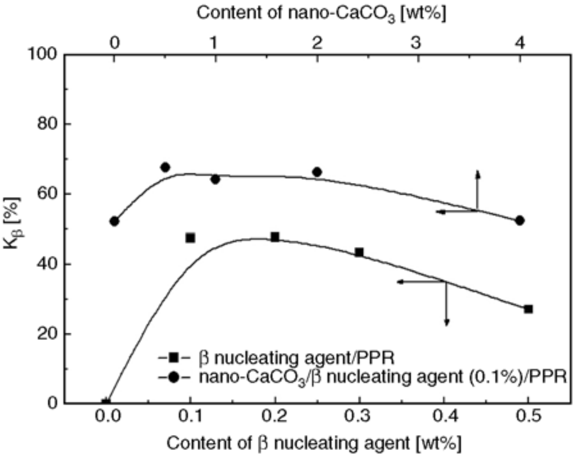

**Figure 3.** Relative amount of β crystal, $K_\beta$, of PPR as a function of contents of β nucleating agent and nano-$CaCO_3$

Clearly, $K_\beta$ increases with a rise in content of β-nucleating agent, and reaches the maximum of 48.0% when the content of β-nucleating agent is around 0.1–0.15 wt%. Further increase of concentration of β-nucleating agent leads to slight reduction in $K_\beta$. The lowering the β-form content with increasing concentration of the β-nucleating agent might be ascribed to the dual nucleating ability of rare-earth typed β-nucleating agent [33, 34], on the surface of which formation of α- and β-phase takes place. A similar phenomenon of the 'critical' content of nucleating agent was observed by Varga and Menyhárd [35]. In the case of constant content of β-nucleating agent of 0.1 wt%, the incorporation of nano-$CaCO_3$ can further increase $K_\beta$ (Figure 3), manifesting that β-nucleating agent and nano-$CaCO_3$ have a synergistic effect on the formation of β-crystal. Above WAXD studies show that nano-$CaCO_3$ used has no β-nucleating effect on PPR. The synergistic β-nucleating effect of nanoparticles and β-nucleating agent might be attributed to formation of $CaCO_3$-supported β-nucleator. During processing, the β-nucleating agent is adsorbed and supported on the surface of the $CaCO_3$ nanoparticles due to the polar interaction between rare-earth β-nucleating agent and $CaCO_3$ particles. A monolayer of β-nucleating agent adsorbed on the surface of the $CaCO_3$ particles might be obtained. Because of larger specific surface area of nanoparticles, $CaCO_3$-supported β-nucleator exhibits high β-nucleating efficiency for PPR crystallization. It has been reported that the content of β-phase in iPP nucleated by the nanoparticles supported β-nucleator are higher than that of iPP nucleated by same β-nucleator [36]. $K_\beta$ decreases with the increase of content of nano-$CaCO_3$ owing to enhanced α-phase nucleating ability of nanoparticles. Thus, the content of β-phase can be tuned by tuning composition of β-nucleating agent and nano-$CaCO_3$ particles.

Figure 4 shows optical micrographs of PPR and its composites crystallized under isothermal conditions. Pristine PPR specimen cooled from melt exhibits conventional spherulitic structure with a diameter of ~400 µm or more, and the interfaces between the spherulites are sharp and clear (Figure 4a). The introduction of nano-$CaCO_3$ and/or β-nucleating agent greatly changes crystalline morphology of PPR, including the decrease of spherulites size. A large number of nuclei are induced within short time, accelerating the crystallization of PPR. The resultant spherulites overlapped each other, and hence become much smaller than those in pristine PPR.

It is worth noting that an interesting morphology, spherulites overgrowths onto the smaller crystal core, is observed in β-nucleated PPR or nano-$CaCO_3$/β-nucleated PPR (Figure 4c and 4d). Výchopňová *et al.* [37] reported the same peculiar structure made of β-core and α-crystal overgrowing on it in PP. There are two possibilities for formation of such mixed polymorphic forms. On one hand, β-α growth tran-

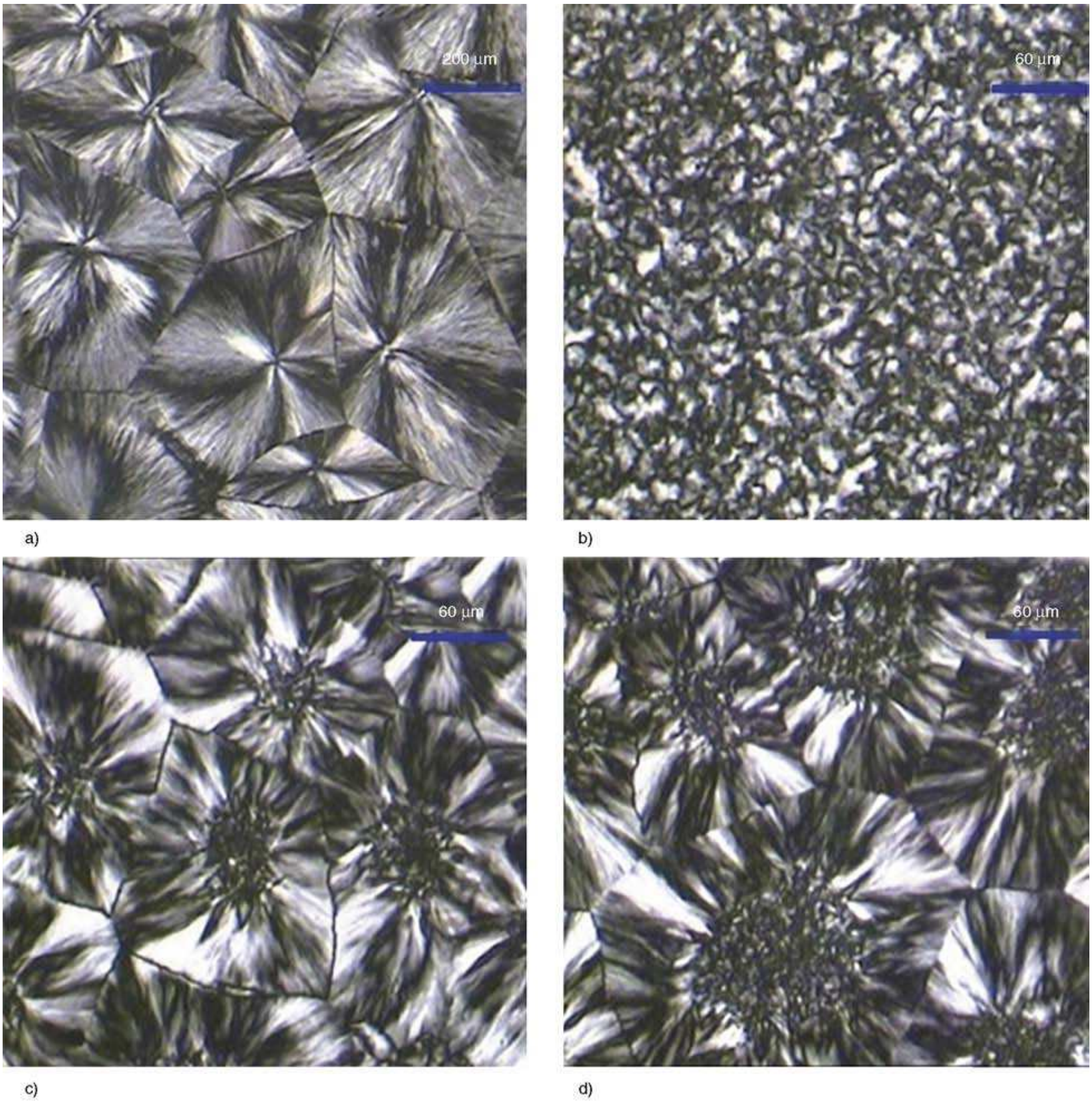

**Figure 4.** Optical micrographs of (a) PPR, (b) nano-$CaCO_3$ (0.5 wt%)/PPR, (c) β nucleated PPR (content of β nucleating agent: 0.1 wt%) and (d) nano-$CaCO_3$ (0.5 wt%)/β nucleated PPR (content of β nucleating agent: 0.1 wt%). Crystallization conditions: 130°C, 16 h.

sition might occur during crystallization of PPR composites. It was reported that β-α growth transition $T_{(\beta\alpha)}$ occurs in the vicinity of 140°C for iPP [38, 39], above where the growth rate of the α-phase ($G_\alpha$) is higher than that of β-phase ($G_\beta$). In the case of random copolymers with low-comonomer content, the β-α growth transition occurs in a wide temperature range because where $G_\alpha$ was always higher than $G_\beta$ for the given random copolymer and even no crossover temperature $T_{(\beta\alpha)}$ was found below which $G_\beta$ would be higher than $G_\alpha$ [21]. Further studies show that the $T_{(\beta\alpha)}$ of random copolymer PP shifts to lower temperatures [23]. Considering thermal condition of crystallization in the study, it is possible that β-α growth transition occurs. One the other hand, polymorphic composition morphology might be connected with the dual nucleating ability of adopted nucleating agent, on the surface of which formation of α- and β-phase takes place. Since in certain temperature range where $G_\alpha$ was always higher than $G_\beta$, such βα twin structure forms.

To confirm the structure of this peculiar crystalline morphology, the sample was slowly heated under optical microscopic observation to check the variation in the morphology (Figure 5). The photographs show that when temperature approaches to 132°C (Figure 5a), crystal cores begin to melt, and the melting is completed at 137°C (Figure 5b). As temperature continues to rise, the outer crystals start to melt at 142°C (Figure 5c), and the melt is com-

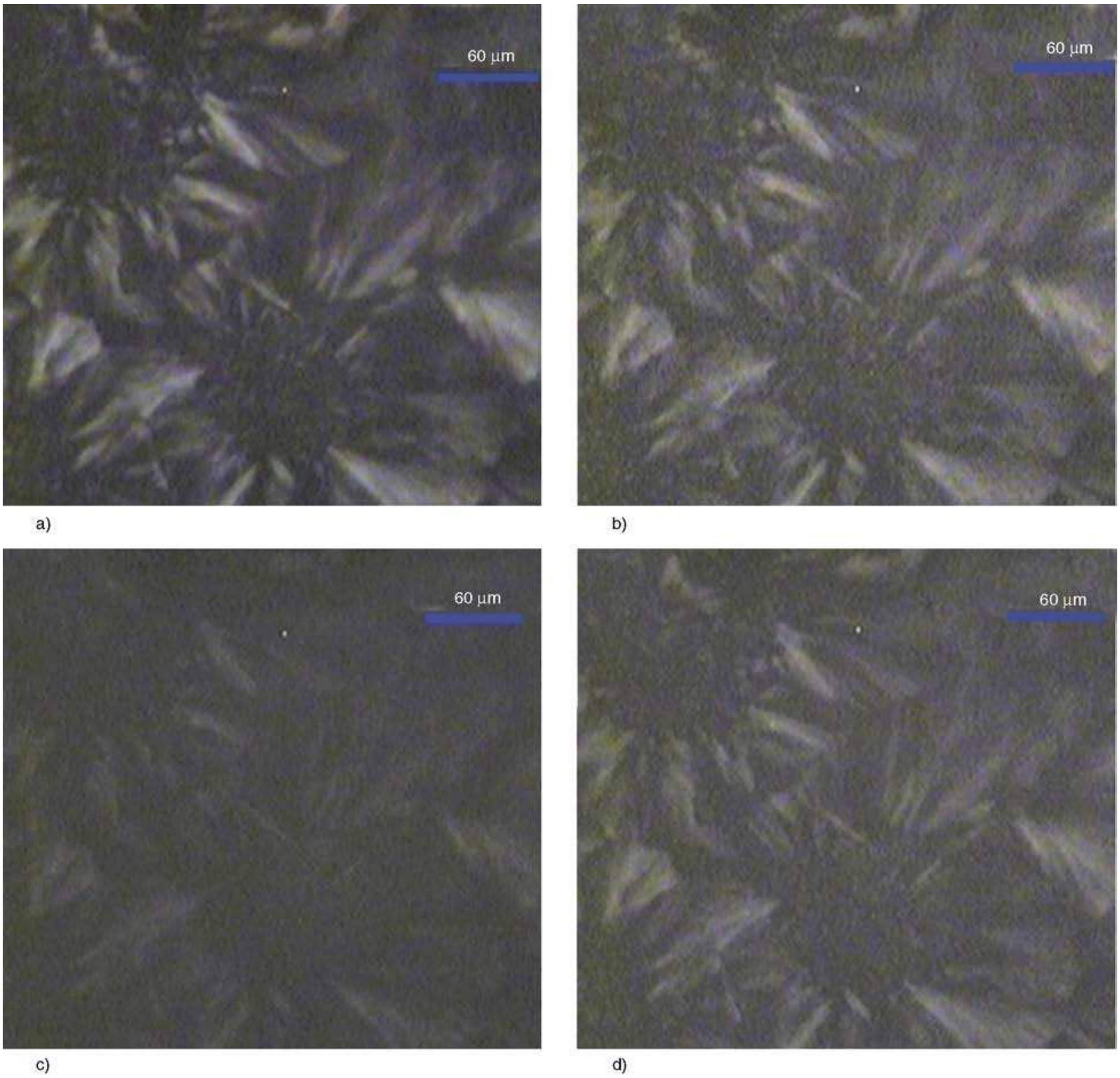

**Figure 5.** Optical micrographs showing melting process of β nucleated PPR (content of β nucleating agent: 0.1 wt%) after crystallization at 130°C for 16 h. Heating rate: 0.1°C/min. (a) 132°C, (b) 137°C, (c) 142°C and (d) 148°C.

pleted at 148°C (Figure 5d). These four critical temperatures exactly fall between β- and α-phase melting peak temperatures tested by DSC (Table 1). Accordingly, composition of this polymorphic structure can be determined. Namely, the core is made of β-phase (also including more or less α-crystal), while α-spherulites grows externally upon the cores.

### 3.3. Mechanical properties

Tensile properties of PPR and its composites are tested and listed in Table 2. Since the addition of β-nucleating agent to PPR induces the formation of β-crystals, Young's modulus and tensile strength of PPR slightly decrease. However, addition of nano-$CaCO_3$ to β-nucleated PPR is able to increase modulus and tensile strength of the system. As a result, the two parameters of nano-$CaCO_3$/β-nucleated PPR composites are close to those of pristine PPR.

With respect to elongation at break and area under tensile stress-strain curve, which is related to static ductility, appearance of β-crystal in PPR certainly increases these two parameters as expected. The PPR composites with nano-$CaCO_3$ exhibit improved static ductility either.

Comparatively, the change in impact strength of the systems due to the incorporation of β-nucleating agent and nano-$CaCO_3$ particles is complicated (Figure 6). β-crystal is always believed to result in improved toughness of PP. As a result, when β-nucleating agent is added, room temperature impact strength of PPR is remarkably increased (Figure 6a). However, the addition of nano-$CaCO_3$ to PPR or to β-nucleated PPR does not obviously alter room temperature impact strength of the composites. The tendency of toughness variation disagrees with the dependence of $K_\beta$ on nano-$CaCO_3$ content (Figure 3). This might be attributed to the fact that nano-$CaCO_3$ particles in PPR containing ethylene units cannot offer sufficient resistance to rapid crack propagation under high speed deformation circum-

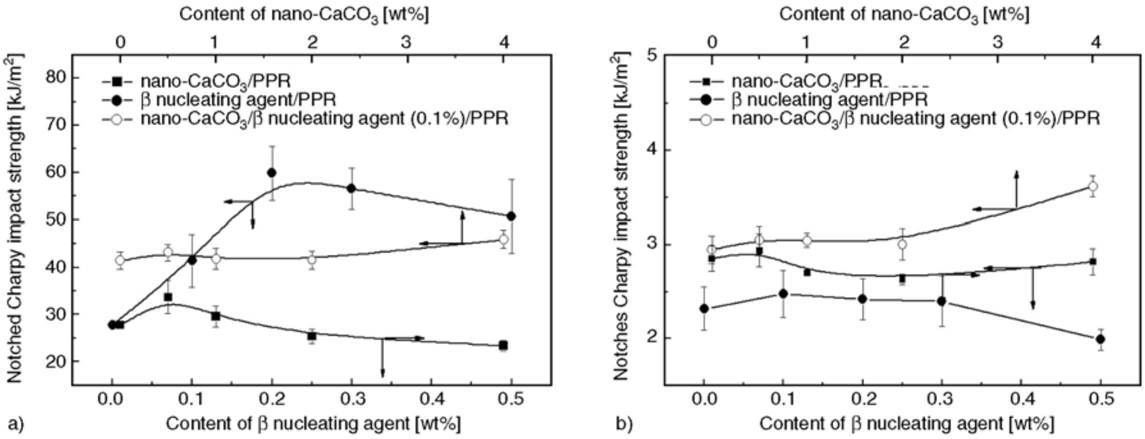

**Figure 6.** Notched Charpy impact strength of PPR as a function of contents of β nucleating agent and nano-$CaCO_3$. Test temperature: (a) 23°C and (b) –10º.

**Table 2.** Tensile properties of PPR and its composites

| Samples | Young' modulus [GPa] | Tensile strength [MPa] | Elongation at break [%] | Area under stress-strain curve [GPa] |
|---|---|---|---|---|
| PPR | 1133.0±35.7 | 52.5±2.4 | 79.8±26 | 9.69±1.04 |
| β-NA (0.1 wt%)/PPR | 1109.0±33.8 | 48.0±2.6 | 80.5±16.1 | 9.71±0.38 |
| β-NA (0.2 wt%)/PPR | 1101.1±37.7 | 47.0±1.4 | 91.3±18.1 | 9.84±0.37 |
| β-NA (0.3 wt%)/PPR | 1102.8±30.1 | 49.0±2.1 | 91.5±24 | 10.88±0.78 |
| β-NA (0.5 wt%)/PPR | 1110.5±31.6 | 45.7±2.3 | 175.9±73 | 11.01±0.73 |
| 0.5 wt% $CaCO_3$/PPR | 1057.4±16.8 | 48.0±1.1 | 123.6±26.8 | 14.15±1.86 |
| 1.0 wt% $CaCO_3$/PPR | 1059.3±18.0 | 47.7±0.3 | 120.8±21.4 | 13.78±1.94 |
| 2.0 wt% $CaCO_3$/PPR | 1094.1±49.9 | 49.3±1.1 | 119.9±46.7 | 13.59±2.37 |
| 4.0 wt% $CaCO_3$/PPR | 1068.9±47.1 | 48.0±1.0 | 116.7±20.6 | 13.19±1.79 |
| Nano-$CaCO_3$ (0.5 wt%)/β-NA (0.1 wt%)/PPR | 1133.4±24.5 | 48.7±0.9 | 89.0±9.8 | 10.96±0.93 |
| Nano-$CaCO_3$ (1.0 wt%)/β-NA (0.1 wt%)/PPR | 1116.2±24.4 | 50.7±1.7 | 87.8±15.3 | 10.77±1.39 |
| Nano-$CaCO_3$ (2.0 wt%)/β-NA (0.1 wt%)/PPR | 1099.1±9.4 | 50.3±0.9 | 79.3±27.5 | 10.65±0.60 |
| Nano-$CaCO_3$ (4.0 wt%)/β-NA (0.1 wt%)/PPR | 1105.8±33.4 | 51.5±0.4 | 102.7±11.8 | 12.09±1.92 |

stances due to poor interfacial adhesion. The case resembles flexible polyethylene filled with nano-$SiO_2$ [40], and the deterioration effect counteracts the toughening effect of β-crystal.

It is interesting to see that when the impact tests are conducted at –10°C, the measured impact strengths of β-nucleated PPR are almost the same as that of pristine PPR (Figure 6b). It means that β-phase fails to take effect at low temperature. However, the addition of nano-$CaCO_3$ improves the low-temperature notched impact strength of PPR, and nano-$CaCO_3$/β-nucleated PPR possesses higher notched impact strength in the case of 4.0 wt% nano-$CaCO_3$. In general, higher loading of nanoparticles would lead to poor dispersion in polymer [41], which disfavors enhancement of room temperature mechanical properties of polymer. Here the abnormal increase in impact strength should be correlated to low temperature characteristics of the composites. Although macromolecular mobility is significantly decreased at –10°C as compared to room temperature, the agglomerated nano-$CaCO_3$ particles might play the role of sandbags [42]. When impact force is applied, relative slip between the nanoparticles inside the agglomerates would take place, which consumes the certain amount of the input mechanical energy. This in turn explains the composites with low nano-$CaCO_3$ content do not show higher impact strength.

Figure 7 gives the results of short-term creep behaviours of PPR and its composites measured at 70°C. We can see that β-nucleated PPR has higher creep strain than pristine PPR, but nano-$CaCO_3$/β-nucleated PPR possesses lower creep strain. The increased creep resistance should result from the hindrance effect of the nanoparticles to polymer chains movement [43]. From a practical point of view, PPR integrated with high temperature creep resistance would extend its service stability in hot water supply and heating pipe system.

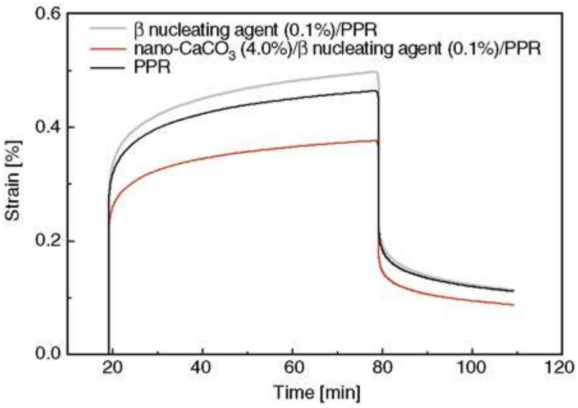

**Figure 7.** Creep behaviors of PPR and its composites tested at 70º under the stress of 1 MPa

## 4. Conclusions

For purposes of tuning properties of PPR, β-nucleated PPR and nano-$CaCO_3$/β-nucleated PPR were prepared by melt compounding. Non-isothermal crystallization and melting behaviors, crystalline morphology and mechanical properties of the materials were investigated. Both β-nucleating agent and nano-$CaCO_3$/β-nucleating agent acted as heterogeneous nucleators in PPR, which was the main reason for the increased total crystallization rate of PPR. In addition, β-nucleating agent and nano-$CaCO_3$ have synergistic effects on β-phase formation of PPR. Moreover, crystalline morphology of PPR became a peculiar βα twin structure made of β-crystal core and α-spherulites outgrowths due to the suitable crystallization temperature and dual nucleating ability of nucleating agent. Compared to pristine PPR, β-nucleated PPR exhibited higher elongation to break and area under tensile stress-strain curve, but lower Young's modulus and tensile strength. By adding nano-$CaCO_3$ particles into β-nucleated PPR, balanced properties can be obtained. Moreover, the composites of nano-$CaCO_3$/β-nucleated PPR possessed improved low temperature impact toughness and high temperature creep resistance.

## Acknowledgements

The authors are grateful for the support of the Natural Science Foundation of China (Grant: 51173207), Sino-Hungarian Scientific and Technological Cooperation Project (Grant: 2009DFA52660), the Natural Science Foundation of Guangdong, China (Grant: 2010B010800020) and Key Laboratory for Nonmetallic Composites and Functional Materials of Sichuan Province (Grant: 2410zxfk24).

## References

[1] Harding G. W., van Reenen A. J.: Fractionation and characterisation of propylene-ethylene random copolymers: Effect of the comonomer on crystallisation of poly(propylene) in the γ-phase. Macromolecular Chemistry and Physics, **207**, 1680–1690 (2006).
DOI: 10.1002/macp.200600242

[2] Stephens C. H., Poon B. C., Ansems P., Chum S. P., Hiltner A., Baer E.: Comparison of propylene/ethylene copolymers prepared with different catalysts. Journal of Applied Polymer Science, **100**, 1651–1658 (2006).
DOI: 10.1002/app.23788

[3] Tjong S. C., Shen J. S., Li R. K. Y.: Impact fracture toughness of β-form polypropylene. Scripta Metallurgica et Materalia, **33**, 503–508 (1995).
DOI: 10.1016/0956-716X(95)00225-K

[4] Karger-Kocsis J., Varga J., Ehrenstein G. W.: Comparison of the fracture and failure behaviour of injection moulded α- and β-polypropylene in high-speed three-point bending tests. Journal of Applied Polymer Science, **64**, 2059–2066 (1997).
DOI: 10.1002/(SICI)1097-4628(19970613)64:11<2057::AID-APP1>3.0.CO;2-I

[5] Karger-Kocsis J., Varga J.: Effects of β-α transformation on the static and dynamic tensile behavior of isotactic polypropylene. Journal of Applied Polymer Science, **62**, 291–300 (1996).
DOI: 10.1002/(SICI)1097-4628(19961010)62:2<291::AID-APP4>3.0.CO;2-S

[6] Varga J., Ehrenstein G. W., Schlarb A. K.: Vibration welding of alpha and beta isotactic polypropylenes: Mechanical properties and structure. Express Polymer Letters, **2**, 148–156 (2008).
DOI: 10.3144/expresspolymlett.2008.20

[7] Grein C.: Toughness of neat, rubber modified and filled β-nucleated polypropylene: From fundamentals to applications. Advances in Polymer Science, **188**, 43–104 (2005).
DOI: 10.1007/b136972

[8] Fujiyama M.: Structures and properties of injection molding of β-crystal nucleator-added polypropylenes. Part 1. Effect of β-crystal nucleator content. International Polymer Processing, **10**, 172–178 (1995).

[9] Fujiyama M.: Structure and properties of injection moldings of β-crystal nucleator-added polypropylene. Part 2, Effect of MFI of base resin. International Polymer Processing, **10**, 251–254 (1995).

[10] Fujiyama M.: Structures and properties of injection moldings of β-crystal nucleator-added polypropylenes. Part 3. Comparison of nucleating effect between γ-quinacridone and quinacridonequinone. International Polymer Processing, **11**, 271–274 (1996).

[11] Lovinger A. J., Chua J. O., Gryte C. C.: Studies on the α and β forms of isotactic polypropylene by crystallization in a temperature gradient. Journal of Polymer Science: Polymer Physics Edition, **15**, 641–656 (1977).
DOI: 10.1002/pol.1977.180150405

[12] Yamamoto Y., Inoue Y., Onai T., Doshu C., Takahashi H., Uehara H.: Deconvolution analyses of differential scanning calorimetry profiles of β-crystallized polypropylenes with synchronized X-ray measurements. Macromolecules, **40**, 2745–2750 (2007).
DOI: 10.1021/ma062784s

[13] Leugering H. J., Kirsch G.: Beeinflussung der Kristallstruktur von isotaktischem Polypropylen durch Kristallisation aus orientierten schmelzen (in German). Die Angewandte Makromolekulare Chemie, **33**, 17–23 (1973).
DOI: 10.1002/apmc.1973.050330102n

[14] Varga J., Karger-Kocsis J.: Rules of supermolecular structure formation in sheared isotactic polypropylene melts. Journal of Polymer Science Part B: Polymer Physics, **34**, 657–670 (1996).
DOI: 10.1002/(SICI)1099-0488(199603)34:4<657::AID-POLB6>3.0.CO;2-N

[15] Varga J.: β-modification of isotactic polypropylene: Preparation, structure, processing, properties, and application. Journal of Macromolecular Science Part B: Physics, **41**, 1121–1171 (2002).
DOI: 10.1081/MB-120013089

[16] Lin Y., Chen H., Chan C-M., Wu J.: High impact toughness polypropylene/$CaCO_3$ nanocomposites and the toughening mechanism. Macromolecules, **41**, 9204–9213 (2008).
DOI: 10.1021/ma801095d

[17] Guo T., Wang L., Zhang A., Cai T.: Effects of nano calcium carbonate modified by a lanthanum compound on the properties of polypropylene. Journal of Applied Polymer Science, **97**, 1154–1160 (2005).
DOI: 10.1002/app.21804

[18] Zhang X., Shi G.: The effect of a β-nucleator on the crystallization and melting behavior of ethylene/propylene random and block copolymers. Thermochimica Acta, **235**, 49–56 (1994).
DOI: 10.1016/0040-6031(94)80082-0

[19] Zhang X., Shi G.: Effect of converting the crystalline form from α to β on the mechanical properties of ethylene/propylene random and block copolymers. Polymer, **35**, 5067–5072 (1994).
DOI: 10.1016/0032-3861(94)90666-1

[20] Sterzynski T., Lambla M., Crozier H., Thomas M.: Structure and properties of nucleated random and block copolymers of propylene. Advances in Polymer Technology, **13**, 25–36 (1994).
DOI: 10.1002/adv.1994.060130102

[21] Varga J., Schulek-Tóth F.: Crystallization, melting and spherulitic structure of β-nucleated random propylene copolymers. Journal of Thermal Analysis, **47**, 941–955 (1996).
DOI: 10.1007/BF01979441

[22] Chen H. B., Karger-Kocsis J., Wu J. S., Varga J.: Fracture toughness of α- and β-phase polypropylene homopolymers and random- and block-copolymers. Polymer, **43**, 6505–6514 (2002).
DOI: 10.1016/S0032-3861(02)00590-6

[23] Juhász P., Varga J., Belina K., Belina G.: Efficiency of β-nucleating agents in propylene/α-olefin copolymers. Journal of Macromolecular Science Part B: Physics, **41**, 1173–1189 (2002).
DOI: 10.1081/MB-120013090

[24] Xiao W., Feng J.: Comparative investigation on crystallization conditions dependence of polymorphs composition for β-nucleated propylene/ethylene copolymer and propylene homopolymer. Journal of Applied Polymer Science, **117**, 3247–3254 (2010).
DOI: 10.1002/app.32229

[25] Na B., Lv R., Xu W., Chen R., Zhao Z., Yi Y.: Effect of nucleating duality on the formation of γ-phase in a β-nucleated isotactic polypropylene copolymer. Polymer International, **57**, 1128–1133 (2008). DOI: 10.1002/pi.2454

[26] Varga J.: β-modification of polypropylene and its two-component systems. Journal of Thermal Analysis and Calorimetry, **35**, 1891–1912 (1989). DOI: 10.1007/BF01911675

[27] Varga J., Schulek-Tóth F.: Filled compounds of the β-modification of polypropylene. Die Angewandte Makromolekulare Chemie, **188**, 11–25 (1991). DOI: 10.1002/apmc.1991.051880102

[28] Labour T., Vigier G., Séguéla R., Gauthier C., Orange G., Bomal Y.: Influence of the β-crystalline phase on the mechanical properties of unfilled and calcium carbonate-filled polypropylene: Ductile cracking and impact behavior. Polymer Science Part B: Polymer Physics, **40**, 31–42 (2002). DOI: 10.1002/polb.10068

[29] Kotek J., Kelnar I., Baldrian J., Raab M.: Tensile behaviour of isotactic polypropylene modified by specific nucleation and active fillers. European Polymer Journal, **40**, 679–684 (2004). DOI: 10.1016/j.eurpolymj.2003.12.004

[30] Gahleitner M., Grein C., Bernreitner K.: Synergistic mechanical effects of calcite micro- and nanoparticles and β-nucleation in polypropylene copolymers. European Polymer Journal, **48**, 49–59 (2012). DOI: 10.1016/j.eurpolymj.2011.10.013

[31] Jeziorny A.: Parameters characterizing the kinetics of the non-isothermal crystallization of poly(ethylene terephthalate) determined by d.s.c. Polymer, **19**, 1142–1144 (1978). DOI: 10.1016/0032-3861(78)90060-5

[32] Turner Jones A., Aizlewood J. M., Beckett D. R.: Crystalline forms of isotactic polypropylene. Macromolecular Chemistry and Physics, **75**, 134–158 (1964). DOI: 10.1002/macp.1964.020750113

[33] Xiao W., Wu P., Feng J., Yao R.: Influence of a novel β-nucleating agent on the structure, morphology, and nonisothermal crystallization behavior of isotactic polypropylene. Journal of Applied Polymer Science, **111**, 1076–1085 (2009). DOI: 10.1002/app.29139

[34] Luo F., Geng C. Z., Wang K., Deng H., Chen F., Fu Q., Na B: New understanding in tuning toughness of β-polypropylene: The role of β-nucleated crystalline morphology. Macromolecules, **42**, 9325–9331 (2009). DOI: 10.1021/ma901651f

[35] Varga J., Menyhárd A: Effect of solubility and nucleating duality of *N*,*N'*-dicyclohexyl-2,6-naphthalenedicarboxamide on the supermolecular structure of isotactic polypropylene. Macromolecules, **40**, 2422–2431 (2007). DOI: 10.1021/ma062815j

[36] Zhang Z., Chen C., Wang C., Zhang J., Mai K.: A novel highly efficient β-nucleating agent for polypropylene using nano-$CaCO_3$ as a support. Polymer International, **59**, 1199–1204 (2010). DOI: 10.1002/pi.2847

[37] Výchopňová J., Habrová V., Čabla R., Obadal M., Čermák R.: The effect of β-nucleation on crystallization behavior of isotactic polypropylene. Proceeding of the 8th Polymers for Advanced Technologies International Symposium. Budapest, Hungary' p.2 (2005).

[38] Varga J.: Supermolecular structure of isotactic polypropylene. Journal of Materials Science, **27**, 2557–2579 (1992). DOI: 10.1007/BF00540671

[39] Varga J., Fujiwara Y., Ille A.: βα-bifurcation of growth during the stepwise crystallization of polypropylene. Periodica Polytechnica Chemical Engineering, **34**, 255–271 (1990).

[40] Zhang M. Q., Rong M. Z., Zhang H. B., Friedrich K.: Mechanical properties of low nano-silica filled high density polyethylene composites. Polymer Engineering and Science, **43**, 490–500 (2003). DOI: 10.1002/pen.10040

[41] Rong M. Z., Zhang M. Q., Zheng Y. X., Zeng H. M., Walter R., Friedrich K.: Structure–property relationships of irradiation grafted nano-inorganic particle filled polypropylene composites. Polymer, **42**, 167–183 (2001). DOI: 10.1016/S0032-3861(00)00325-6

[42] Wang X., Sun J., Huang R.: Influence of the compounding route on the properties of polypropylene/nano-$CaCO_3$/ethylene–propylene–diene terpolymer tercomponent composites. Journal of Applied Polymer Science, **99**, 2268–2272 (2006). DOI: 10.1002/app.22767

[43] Zhou T. H., Ruan W. H., Yang J. L., Rong M. Z., Zhang M. Q., Zhang Z.: A novel route for improving creep resistance of polymers using nanoparticles. Composites Science and Technology, **67**, 2297–2302 (2007). DOI: 10.1016/j.compscitech.2007.01.015